ETHYLENE OXIDE REACTOR DESIGN

Ammar Ali (10773038)

GROUP MA (2025)

Abstract

This report proposes a comprehensive design for a multi-tubular packed-bed ethylene oxide (EO) reactor system, emphasizing high selectivity and safe operation. The design is based on a silver-catalyzed partial oxidation of ethylene at moderate per-pass conversion (~10 %) to preserve overall selectivity at ~85 %. Kinetic modeling, informed by Langmuir–Hinshelwood-type rate expressions and incorporating low-level inhibitor (1–2 ppm dichloroethane), indicates that elevated temperatures and oxygen partial pressures must be carefully balanced to maintain high EO yield while preventing complete oxidation. A parametric study explores how varying the inlet temperature, coolant conditions, pressure, and inhibitor concentration affects conversion, selectivity, and hotspot formation. Results confirm that a tightly controlled operating window—maintaining reactor temperatures near 220–230 °C and feed pressures at around 20–21 atm—achieves stable production without risking thermal runaway. Mechanical design calculations and sizing for ancillary equipment, including preheaters and steam-generating boilers, ensure sufficient heat removal and compliance with ASME standards. Recommendations for refining the model include explicitly modeling catalyst deactivation, exploring radial temperature gradients, and adopting advanced process control strategies. Overall, the reactor design fulfills key industry objectives: moderate single-pass conversion, robust control over exothermicity, and consistently high selectivity toward ethylene oxide.

Declaration of Authorship

No part of the work referred to in this report has been submitted in support of an application for any Degree or other qualification at this or any other university or other institute of learning.

Signed: …… 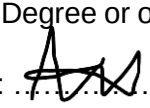 …

Table of Contents

1 Introductory Context

Ethylene oxide (EO) is a critical intermediate in the chemical industry, used in the production of surfactants, solvents, and a variety of ethylene-glycol-based products. Globally, EO production exceeds several million tonnes per year, with demand continuously growing due to its role in manufacturing polymers, detergents, and other essential chemicals (Kirk and Othmer, 2005). Industrial production of EO typically employs the partial oxidation of ethylene over silver-based catalysts in multi-tubular packed-bed reactors. These reactors provide efficient heat management and high selectivity, mitigating the risk of runaway reactions in what is otherwise a highly exothermic process. Commercial plants commonly operate at pressures of about 18–22 atm, with gas inlet temperatures 170 – 210 °C and coolant temperatures around 220 °C (Nawaz, 2016) (Kirk and Othmer, 2005).

This report details the design of the packed bed reactor and its auxiliary equipment's in the ethylene oxide (EO) production process. In this process, the partial oxidation of ethylene is desired and promoted, whilst simultaneously ensuring the complete oxidation of ethylene is limited. The three main reaction that will occur in the ethylene oxide reactor are presented in Equations 1.1 to 1.3. Equation 1.1 is the desired reaction and Equations 1.2 and 1.3 are undesired parallel and series reactions respectively. (Petrov, Eliyas and Shopov, 1985)

$$C_2H_4 + \frac{1}{2}O_2 \longrightarrow C_2H_4O \qquad \Delta H_{r_1} = -105\frac{kJ}{mol} \qquad \text{Equation 1.1}$$

$$C_2H_4 + 3\,O_2 \longrightarrow 2\,CO_2 + 2\,H_2O \qquad \Delta H_{r_2} = -1324\frac{kJ}{mol} \qquad \text{Equation 1.2}$$

$$C_2H_4O + \frac{5}{2}O_2 \longrightarrow 2\,CO_2 + 2\,H_2O \qquad \Delta H_{r_3} = -1219\frac{kJ}{mol} \qquad \text{Equation 1.3}$$

1.1 Design Objectives and Constraints

This report focuses on designing the reactor section of a plant intended to produce approximately 164 kt yr^{-1} of EO (continuous production rate of ~129 mol s^{-1} EO). Previous analyses estimated an ethylene per-pass conversion of ~10% and a selectivity of ~85% toward EO (Kirk and Othmer, 2005). These values guide the key objectives:

1. Achieve Desired Conversion and Selectivity
    - Conversion of ethylene ~10% per pass.
    - Selectivity toward EO ~85%.
2. Ensure Operational Safety
    - Avoid runaway conditions in an exothermic partial oxidation.
    - Maintain the oxygen concentration below ~9 mol % to minimise flammability risks.
    - Limit feed and reactor temperatures to avoid thermal decomposition of EO and formation of hotspots.
3. Maintain Reliability and Economic Feasibility
    - Align with industry-standard designs for EO reactors.

- Consider practical operating conditions and materials that minimise both hazards and overall cost.

Given that the undesired total oxidation reactions (Equations 1.2 and 1.3) release significantly more heat than the desired partial oxidation of ethylene (Equation 1.1), managing heat effectively is a top priority. Excess heat not only lowers selectivity (because EO can further oxidise to CO_2 and H_2O) but also raises the risk of thermal runaway. Consequently, the reactor design must be optimised to balance production rates with safe operating limits.

1.2 Unit selection and Justification

Given that the process is continuous and is heterogenous (with a gas phase feed and solid phase catalyst), there are three types of reactors that can be considered; the packed bed tubular reactor (PBR), fluidised bed reactor (FBR) and continuous stirred tank reactor (CSTR).

The PBR design contains many tubes packed with a silver catalyst. A cooling medium (e.g. hot oil) in the shell side removes heat, keeping the reaction near isothermal. This is the standard in EO production due to proven selectivity, large heat-transfer area, and ease of scale-up.

An FBR Could provide good heat transfer, but silver catalysts are not commonly used in fluidized form for EO due to the catalyst deactivation from attrition (Nawaz, 2016). The attrition of catalyst and the complexities of handling O_2 in fluid bed are significant.

CSTRs are not typically used for highly exothermic, gas-phase partial oxidations with solid catalyst because controlling temperature and handling the catalyst is more difficult. A multi-phase fluid would be needed (gas + solid catalyst), with potential for poor selectivity.

Based on industry practice, partial oxidation to EO is nearly always done in a multi-tubular PBR with an external coolant, often referred to as a “shell-and-tube reactor,” with catalyst pellets inside thousands of narrow tubes (Peschel et al., 2011)(Galan et al., 2009)(Berg, 2025). This design ensures consistent temperature control and minimal risk of flammable hot spots. It also allows stable operation at high pressure and moderate temperature.

Thus, the packed bed (multi-tubular) reactor is selected.

1.3 Additional Preliminary Considerations

1.3.1 Catalyst

The activity and selectivity of ethylene oxide production rely heavily on the properties of the silver catalyst loaded within the tubes. In commercial practice, silver is typically dispersed on an α-alumina support whose physical characteristics such as surface area, pore distribution, and mechanical strength have been optimised over decades of industrial experience. The inherent advantage of silver lies in its ability to favour epoxidation over complete oxidation when contacted with ethylene and oxygen. (Fazeli, Naseri and Eslamjamal, 2020)(Berg, 2025)

In many modern catalysts, promoters or dopants are added to the silver particles to steer reaction pathways and suppress the undesired combustion route to carbon dioxide. These promoters can also affect the formation or removal of surface oxygen species responsible for further oxidation of EO to CO_2.

The physical form of the alumina pellets themselves often cylindrical pellets, rings, or spherical beads helps balance pressure drop through the tube and the diffusion of reactants. Particle

diameter typically varies between 3 mm and 10 mm (Nawaz, 2016), with smaller particles offering more surface area but potentially generating higher pressure drops if packed too densely.

Manufacturers often engineer catalysts to include a thin shell of silver on the outer portion of the support particles, leaving the core mainly inert. This design approach ensures that reactants can access the active silver without requiring deep pore diffusion, thereby reducing mass-transfer limitations.

Catalyst deactivation over time can result from chlorine-induced surface changes, carbonaceous deposits, or sintering of silver particles at high temperatures. Employing an inhibitor such as 1,2-dichloroethane (DCE) helps to minimise side reactions, but if used in excessive quantities, it can cause deactivation by over-chlorinating the silver sites. In this design an DCE inhibitor is used and is discussed in the following sections (Petrov et al., 1988).

In practice, catalyst replacement is carried out on a planned schedule. The used catalyst can be regenerated or reprocessed, with silver often recovered and recycled to reduce costs. Operational parameters, such as feed composition, oxygen concentration, reactor temperature, and inhibitor dosage, are periodically fine-tuned to extend catalyst life, maintain selectivity, and manage conversion per pass. The choice of a particular catalyst formulation thus reflects a balance between upfront cost, anticipated lifespan under expected process conditions, and alignment with the plant's overall process design and safety requirements (Aryana et al., 2009).

1.3.2 Inhibitor (DCE)

The addition of 1,2-dichloroethane (DCE) in small concentrations, often measured in parts per million, can significantly enhance ethylene oxide selectivity by inhibiting deep oxidation pathways. Although silver catalysts inherently favour the formation of EO over CO_2, side reactions become more prevalent under higher operating temperatures and pressures. Chlorine species derived from DCE adsorb onto the silver surface, modifying the electronic environment and blocking adsorption sites that would otherwise facilitate full combustion. This mechanism helps sustain an epoxidation route, improving yields of EO while reducing the consumption of ethylene toward complete oxidation products (Petrov, Eliyas and Shopov, 1986).

Optimising the DCE dosage is a balancing act. When maintained in the range of about 1–2 ppm, DCE is often sufficient to suppress total oxidation without adversely affecting catalyst performance. If concentrations exceed this narrow window, an overabundance of chlorine on the catalyst surface can lead to accelerated deactivation. In such scenarios, the active sites on silver can become partially poisoned, reducing both catalyst activity and overall EO productivity. Plant operators typically install continuous monitoring instruments or periodic sampling procedures in the feed lines to verify DCE concentration levels, and they adjust feed injection rates in response to real-time conditions (Galan et al., 2009). This dynamic control loop is particularly important because variations in the feed composition, overall reaction rate, or bed temperature can shift the catalyst's sensitivity to chlorine.

Although some research has investigated alternative chloro-organic additives or promoters, DCE remains the most commonly employed inhibitor for partial oxidation to EO (Berg, 2025). The tight tolerances on its concentration illustrate the delicate nature of epoxidation chemistry, where even minor process deviations can shift the reaction away from the highly selective formation of ethylene oxide.

1.3.3 Material selection

A robust material of construction for ethylene oxide reactors must withstand elevated temperatures, moderate-to-high pressures, and the chemical reactivity of EO. Stainless steel remains the foremost choice due to its corrosion resistance and stability in environments where trace acids, moisture, or oxygen could otherwise induce unwanted side reactions (Nawaz, 2016). Unlike carbon steel, which may require extensive pretreatment and rigorous control of rust or scaling, stainless steel offers an innate protective oxide layer that mitigates many typical corrosion mechanisms. Additionally, the presence of oxygen and the possibility of minor impurities in the feed necessitate a material that can handle oxidative conditions without forming catalytic sites that lead to EO polymerization.

Among the stainless steel grades, 304L and 316L stand out for their balance of cost, weldability, and corrosion resistance. However, 316L is frequently selected for the high-pressure zones of the reactor because its molybdenum content confers greater resistance to pitting and crevice corrosion (Smith, 2022).

Although certain upstream or downstream sections of the plant might safely employ carbon steel, the internal tubes of the reactor demand stainless grades to safeguard against the undesirable reactivity or contamination that can occur if EO comes into direct contact with less resistant metals. Overextended contact between ethylene oxide and certain metals like copper and zinc can foster the formation of acetylides or other explosive compounds, a risk mitigated by excluding these metals or by ensuring that any copper- or zinc-containing lines are thoroughly passivated and kept free from moisture.

1.4 Flow Diagram and Stream Table

A simplified flow diagram (Figure 1.1) represents the reactor feed preparation and the multi-tubular reactor itself. Table 1.1 shows the stream data from the preliminary design in part 1.

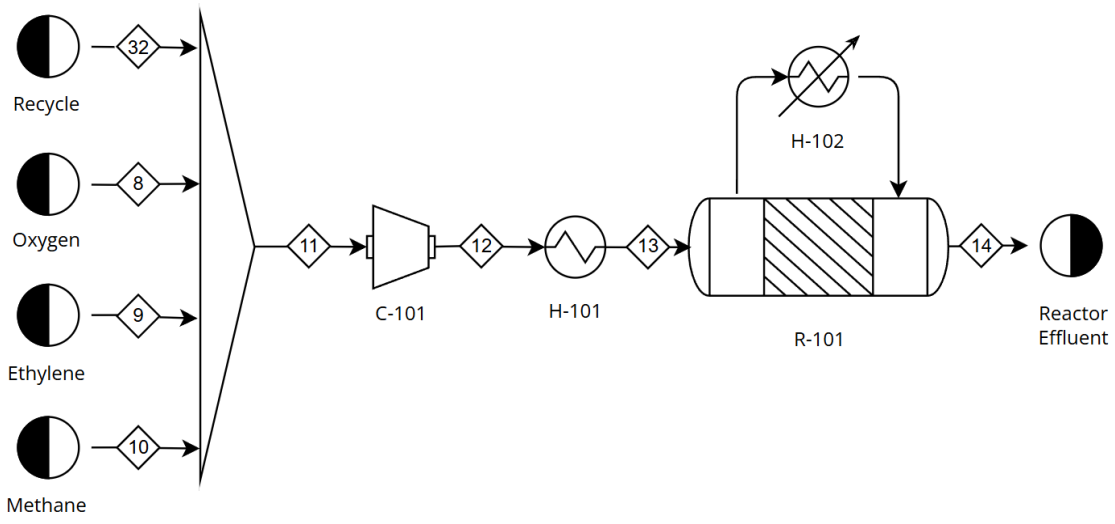

Figure 1.1 – Simplified process flow diagram

Table 1.1 – Stream table from preliminary design

Stream	8	9	10	11	12	13 (Feed)	14	32
Vapour Mole Fraction	1	1	1	1	1	1	1	1
Temperature (^{O}C)	50	50	50	58	58	230	230	64
Pressure (atm)	21	21	21	21	21	21	21	21
Molar Flowrate (mol s^{-1})	142	167	56	8800	8800	8800	8750	8444
Molar Fraction								
C2H4	0	1	0	0.173	0.173	0.173	0.157	0.161
EO	0	0	0	0.0001	0.0001	0.0001	0.015	0.0001
CH4	0	0	1	0.675	0.675	0.675	0.679	0.697
CO2	0	0	0	0.029	0.029	0.029	0.034	0.030
H2O	0	0	0	0.005	0.005	0.005	0.011	0.006
Ar	0.02	0	0	0.035	0.035	0.035	0.035	0.036
O2	0.98	0	0	0.084	0.084	0.084	0.070	0.071

2 Methodology

2.1 Design Procedure

A simplified five-step procedure outline by Towler and Sinnott (2012) was followed:

1. Data Collection
   Gathered kinetic, thermodynamic, and physical property data from literature and standard databases (e.g., NIST WebBook, vendor data for coolant properties).

2. Rate-Controlling Mechanism
   Assessed whether the reactor is primarily kinetically controlled or significantly influenced by mass/heat transfer. Due to the small tube diameters commonly used in EO reactors, the system often approximates a plug-flow regime with minimal radial gradients (assuming proper design).

3. Initial Model and Parameters
   Proposed reactor operating conditions (e.g., temperature, pressure, residence time) to meet the targeted ethylene conversion (~10%) and EO selectivity (~85%). Also incorporated constraints on oxygen concentration, inlet temperature, and DCE inhibitor levels to mitigate runaway risk.

4. Reactor Sizing and Performance Estimation
   Developed mass and energy balance equations, along with kinetic expressions, to size the reactor (length, diameter, number of tubes) and predict temperature/conversion profiles.

5. Iterative Evaluation
   Although a full economic optimization was not performed, a rudimentary sensitivity

analysis helped refine key variables such as reactor length, coolant temperature, and inlet pressure.

2.2 Design Assumptions

Table 2.1 summarises the major assumptions used in the reactor model. These assumptions stem from typical multi-tubular packed-bed reactor design practices for ethylene epoxidation and simplify the complex fluid-flow and reaction phenomena.

Table 2.1 - Summary of main design assumptions

Assumption	Justification
1. Uniform radial concentration & temperature (1D plug flow)	Tube diameters are relatively small (e.g., 3–5 cm) compared to length. Heat transfer and radial mixing are sufficient to assume negligible radial gradients. (Aryana et al., 2009)
2. Negligible mass-transfer resistance (gas to catalyst)	Typically, external film mass transfer is fast relative to the intrinsic reaction kinetics, especially with small catalyst pellets and moderate gas velocities. (Aryana et al., 2009) (Galan et al., 2009)
3. Axial diffusion negligible	Convection in the axial direction is far stronger than axial diffusion for typical EO reactor velocities, justifying a plug-flow assumption. (Aryana et al., 2009) (Galan et al., 2009)
4. Constant bed porosity	Catalyst pellets are uniformly packed; minor variations in porosity are neglected.
5. Ideal gas behavior	Pressures are in the range 18–21 atm, and temperatures around 200–300 °C. While not extremely high, real-gas corrections could be minor, but the ideal gas assumption is a common simplification for design-phase calculations.
6. Negligible catalyst–wall heat-transfer resistance	The contact area between the catalyst and tube wall is assumed to be negligible, therefore the heat transfer between the two regions is not modelled. (Galan et al., 2009) (Aryana et al., 2009)
7. Steady-state operation	Dynamic effects (startup, shutdown, transient changes) are not modelled.
8. Co-current cooling in the packed bed reactor	Co-current cooling is desirable due to the coolant having three purposes in the reactor jacket. Namely, to preheat the gas feed in the inert inlet section, maintain a stable temperature in the catalyst section and to cool down reactor effluent in the inert outlet section of the reactor. The graph in Figure 4.3 illustrates this.

2.3 Physiochemical properties

Accurate estimation of thermophysical properties is crucial to the reactor's material and energy balances. In this section, the property models used for each species and for the coolant fluid is outlined.

2.3.1 Heat capacity

The Shomate equation (National Institute of Standards and Technology, 1997) was used to represent the temperature dependence of the heat capacities of key species (C_2H_4, O_2, CO_2, H_2O, and EO). It has the general form shown in Equation 2.1.

$$C_{p,i} = A_{cp,i} + B_{cp,i}T_g + C_{cp,i}T_g^2 + D_{cp,i}T_g^3 + \frac{E_{cp,i}}{T_g^2} \quad \text{Equation 2.1}$$

where T_g is the absolute temperature of the gas (K), and $A_{cp,i}$, $B_{cp,i}$,… are species-specific coefficients taken from NIST.

The heat capacity of stainless steel 316L is given by Equation 2.2 (S. Kim, 1975)

$$C_{p,w} = 0.1097 + 3.174 \times 10^{-5} T_w \quad \text{Equation 2.2}$$

where T_w is the absolute temperature of the metal wall (K)

The heat capacity of the coolant was based of the heat capacity of the heat transfer fluid, Therminol 55, sold by Eastman Chemical Company. At an average coolant temperature of 220 °C, a heat capacity of 2610 J kg^{-1} K^{-1} is given (Eastman Chemical Company, 2015).

2.3.2 Viscosity

Gas viscosities were estimated via Sutherland's formula (White, 2006) which for species i has the form:

$$\mu_i(T_g) = \mu_{i,0} \left(\frac{T_g}{T_{g,0}} \right)^{3/2} \frac{T_0 + S_{\mu,i}}{T_g + S_{\mu,i}} \quad \text{Equation 2.3}$$

where $\mu_{i,0}$, $T_{g,0}$ and $S_{\mu,i}$ are reference parameters. A mean viscosity for the gas mixture was then calculated

The viscosity of the coolant (Therminol 55) was approximated at an average temperature of 220 °C at 6.25x10^{-5} based on vendor data.

2.3.3 Thermal conductivity

Thermal conductivity can also be approximated using Sunderland's formula given in Equation 2.4 (White, 2006)

$$\lambda_i(T_g) = \lambda_{i,0} \left(\frac{T_g}{T_{g,0}} \right)^{3/2} \frac{T_0 + S_{\lambda,i}}{T_g + S_{\lambda,i}} \quad \text{Equation 2.4}$$

The thermal conductivity of stainless steel 316L was approximated at 500 K to be 17.1 W m^{-1} K^{-1} (S. Kim, 1975).

The thermal conductivity of the coolant Therminol 55 was approximately 0.105 W m^{-1} K^{-1} (Eastman Chemical Company, 2015)

3 Detailed Chemical Engineering Design

This section presents the detailed reactor model for the ethylene oxide (EO) process, building on the physical properties and design assumptions introduced in Section 2. The model includes kinetics and stoichiometry, an energy balance, heat-transfer correlations, and an evaluation of pressure drop. Together, these elements allow for an in-depth assessment of reactor performance under the specified operating conditions.

3.1 Kinetics and Stoichiometry

The literature contains numerous kinetic models for ethylene epoxidation, each with strengths and weaknesses (Fazeli, Naseri and Eslamjamal, 2020). For this design, we adopt the Petrov (1985, 1986, 1988) model, which:

- Accounts for both the oxidation of ethylene and the further oxidation of EO itself.
- Includes inhibitory effects of the DCE additive.

This model is defined by a set of reaction rate expressions (Equations 3.1–3.3) in partial pressures of ethylene, oxygen, EO, and DCE. The original forms (in mol g^{-1} h^{-1}) are adapted here to an industrial scale (mol m^{-3} s^{-1}) using Equation 3.5.

$$r_1 = \frac{k_1 P_{O_2} P_{C_2H_4} - k_2 P_{O_2} P_{C_2H_4} P_{DCE}^{0.19}}{1 + k_5 P_{O_2} + k_6 P_{C_2H_4}} \quad \text{Equation 3.1}$$

$$r_2 = \frac{k_3 P_{O_2} P_{C_2H_4} - k_4 P_{O_2} P_{C_2H_4} P_{DCE}^{0.07}}{1 + k_5 P_{O_2} + k_6 P_{C_2H_4}} \quad \text{Equation 3.2}$$

$$r_3 = \frac{k_7 P_{O_2} P_{C_2H_4O} - k_8 P_{O_2} P_{C_2H_4O} P_{DCE}^{0.58}}{(1 + k_9 P_{O_2} + k_{10} P_{O_2}^{0.5} + k_{11} P_{C_2H_4O} + k_{12} P_{C_2H_4O} P_{O_2}^{-0.5})^2} \quad \text{Equation 3.3}$$

$$k_j = A_j e^{-\frac{E_{A,j}}{R T_s}} \quad \text{Equation 3.4}$$

where P_i is the partial pressure of species i (atm), R is the gas constant 8.314 J mol^{-1} K^{-1}, T_s is the catalyst surface temperature (K), and $A_j, E_{A,j}$ are pre-exponential factors and activation energies, respectively, from Petrov, Eliyas and Shopov (1985, 1986)

$$\hat{r_i} = r_i \rho_s (1 - \varepsilon) \times \frac{1000}{3600} \quad \text{Equation 3.5}$$

where ρ_s is the bulk catalyst density (kg m^{-3}), ε is the bed void fraction, and the numeric constants (1000 and 3600) handle unit conversions (e.g., from kg to g, hours to seconds).

3.2 Energy balance and heat transfer

Achieving high EO selectivity in a highly exothermic system requires careful thermal management. This section outlines the energy balance equations, along with key heat transfer correlations used to compute the temperature profile in the reactor tubes and shell-side coolant.

3.2.1 Energy balance

Following Galan et al. (2009) typical heterogenous packed-bed reactor modelling, we write separate energy balances for the solid catalyst (Equation 3.6), gas (Equation 3.7), and coolant (Equation 3.8). Assuming:

- Steady-state, 1D flow.
- Negligible radial temperature gradients (Section 2 assumptions).
- Uniform catalyst temperature in each cross-section.

- Co-current coolant flow

$$\sum_{i=1}^{R} \hat{r}_i \left(-\Delta H_{\mathrm{rxn},i}\right) = h_s\, a_s \left(T_s - T_g\right) \qquad \text{Equation 3.6}$$

where $\hat{r}_i$ is the rate of reaction i (mol m⁻³ s⁻¹), $-\Delta H_{\mathrm{rxn},i}$ is the heat of reaction i (J mol⁻¹), h_s is the particle–gas heat-transfer coefficient, and a_s is the effective interfacial area per unit volume of bed.

$$\frac{dT_g}{dz} = \frac{1}{\rho_g\, C_{p,g} v_g} \left[h_s\, a_s \left(T_s - T_g\right) - \frac{4U}{d_i} \left(T_g - T_c\right)\right] \qquad \text{Equation 3.7}$$

with v_g the superficial gas velocity, ρ_g the gas density, $C_{p,g}$ the gas-phase heat capacity, and U the overall heat-transfer coefficient from the tube side to the shell-side coolant. Here, T_c is the coolant temperature, and d_i is the tube inner diameter.

$$\frac{dT_c}{dz} = \frac{4U}{\rho_c\, C_{p,c} v_c} \frac{N_t\, d_o}{\left(d_{shell}^2 - N_t\, d_o^2\right)} \left(T_g - T_c\right) \qquad \text{Equation 3.8}$$

where d_o is the tube outer diameter, ρ_c and $C_{p,c}$ are the coolant density and heat capacity, and v_c is the coolant volumetric flowrate. The number of tubes is given by N_t.

3.2.2 Heat transfer correlations

The diagram in Figure 3.1 shows the different heat transfer resistances that need to be accounted for in the model. The correlations used to find the coefficients are shown in Equations 3.9 – 3.14 (Galan et al., 2009).

$$N_{\mathrm{Re},c} = \frac{G_c\,(d_s^2 - N_\mathrm{t}\,d_o^2)}{\mu_c\,d_s} \qquad \text{Equation 3.9}$$

$$N_{\mathrm{Pr},c} = \frac{C_{p,c}\,\mu_c}{\lambda_c} \qquad \text{Equation 3.10}$$

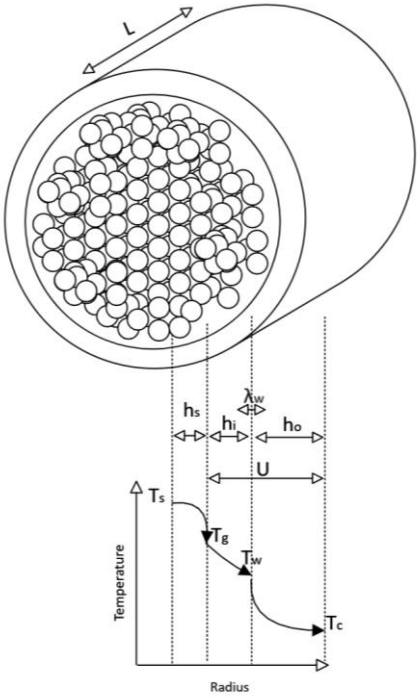

Figure 3.1 – Diagram of a reactor tube showing location of heat transfer resistance and temperature profile

$$h_s = \left(\frac{C_{p,g}\mu_g}{\lambda_g}\right)^{-0.67}\left(\frac{2.867}{N_{\mathrm{Re},p}} + \frac{0.3023}{N_{\mathrm{Re},p}^{0.35}}\right)\rho_g\,C_{p,g}\,v_g \qquad \text{Equation 3.11}$$

$$h_i = 7.676 + 0.0279\,\frac{\lambda_g}{d_p}\,N_{\mathrm{Re},p} \qquad \text{Equation 3.12}$$

$$h_o = 0.023\,N_{\mathrm{Re},c}^{-0.2}\,N_{\mathrm{Pr},c}^{-0.6}\,\rho_c\,C_{p,c}\,v_c \qquad \text{Equation 3.13}$$

$$\frac{1}{U} = \frac{1}{h_i} + \frac{d_o - d_i}{2\,\lambda_w} + \frac{1}{h_o} \qquad \text{Equation 3.14}$$

where $N_{\mathrm{Re},p}$ is the Reynolds number based on particle diameter d_p and gas velocity v_g. λ is the thermal conductivity.

3.3 Pressure Drop

The gas mixture flows through a packed bed of catalyst pellets, incurring a pressure drop along the tube length. The Ergun equation (Equation 3.15) (White, 2006) is the standard correlation for packed-bed pressure drop.

$$-\frac{dP}{dz} = 150\,\frac{\mu_g\,(1-\varepsilon)^2}{\varepsilon^3\,d_p^2}\,v + 1.75\,\frac{\rho_g\,(1-\varepsilon)}{\varepsilon^3\,d_p}\,v^2 \qquad \text{Equation 3.15}$$

where μ_g is gas viscosity, ε is bed void fraction, d_p is particle diameter, and v is the superficial velocity. The first term captures viscous losses, and the second term captures inertial losses. For large-scale EO reactors, the pressure drop is often moderate (~1–2 atm) but must be carefully accounted for in design to ensure stable operation and to size upstream compressors correctly.

4 Parametric Study

The equations and physical properties outlined in Section 2 and 3 were implemented in a Python program. Initial values for variables outlined in Table 4.1 were used to create a base case model that approximately meets the objectives of the reactor section (83.8% selectivity and 10.2% conversion of ethylene). The result from the base case shown in Figures 4.1 – 4.3 also show that the base case design is reasonable as the temperature and pressure ranges are within an acceptable range.

A parametric study was then conducted on the certain variables to further optimise the design of the reactor as well as providing an understanding of the operating range of the reactor.

Table 4.1 – Reactor parameters values (Nawaz, 2016)

Model Variable	Symbol	Value	Units
Reactor inert length	L_{inert}	1	m
Reaction zone length	L_r	12	m
Total reactor length	L_{tot}	14	m
Tube inner diameter	D_{in}	0.045	m
Tube outer diameter	D_{out}	0.05	m
Shell diameter	D_{shell}	8	m
Inlet pressure	P_{in}	21.0	atm
Inlet gas temperature	$T_{g,in}$	210.0	°C
Inlet coolant temperature	$T_{c,in}$	220.0	°C
Total molar flowrate	F_{total}	8800	mol s-1
Number of tubes	N_{tubes}	25,000	–
Molar flowrate per tube	F_{in}	0.352	mol s-1
Coolant mass flow rate	$\dot{m}_c$	2000	kg/s

Table 4.2 – Catalyst parameter values (Nawaz, 2016)

Model Variable	Symbol	Value	Units
Bulk catalyst density	ρ_{bulk}	1260.0	kg/m³
Void fraction	ε	0.45	–
Catalyst particle diameter	d_{cat}	0.006	m
Interfacial area	a_i	$6\frac{1-\varepsilon}{d_{cat}}$	m²/m³

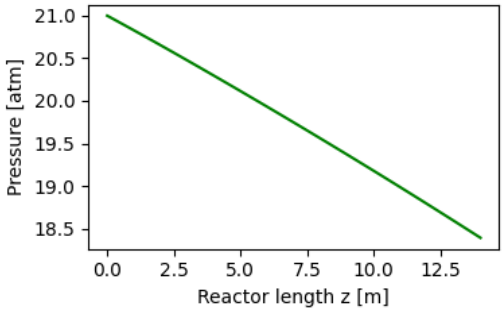

Figure 4.1 – Pressure profile of reactor

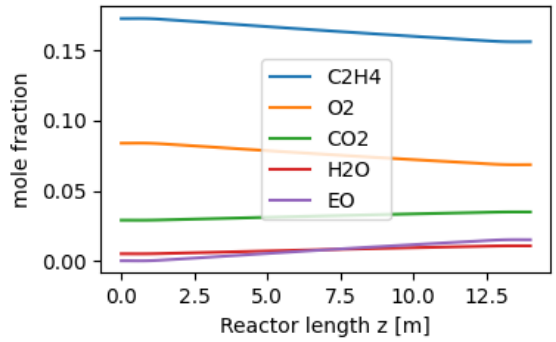

Figure 4.2 – Species profile of reactor

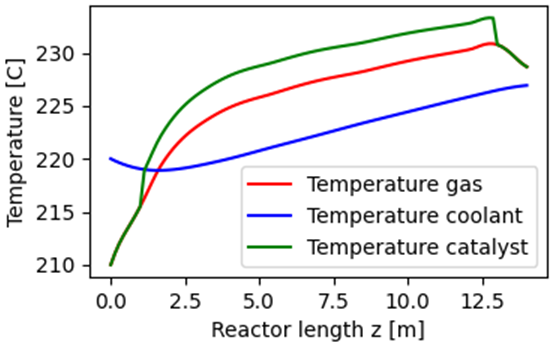

Figure 4.3 – Temperature profile of reactor

After establishing the base case model, a parametric study was conducted using Monte Carlo simulations. Five operating variables and design parameters outlined in Table 4.3 were used in the study. Random parameter values within the ranges outlined in Table 4.3 were generated and then simulated in the Python model. The conversion and selectivity of the simulations were then plotted in each Figure 4.4-4.8. The respective colour bar in each figure allows the trend in selectivity and conversion to be seen. A summary of each trend and key takeaways from the analysis can be found in Table 4.4

Table 4.3 – List of variables and selection ranges in parametric study

Variable Investigated	**Variable selection range in parametric study**
Coolant temperature	180 °C – 250 °C
Gas inlet temperature	180 °C – 250 °C
Reactor length (catalyst section only)	5 m – 15 m
Number of tubes	20,000 – 30,000
Inlet pressure	15 atm – 25 atm

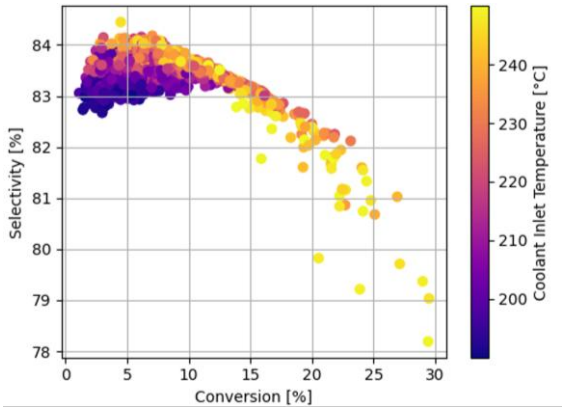

Figure 4.4 – Effect of coolant temperature on conversion and selectivity

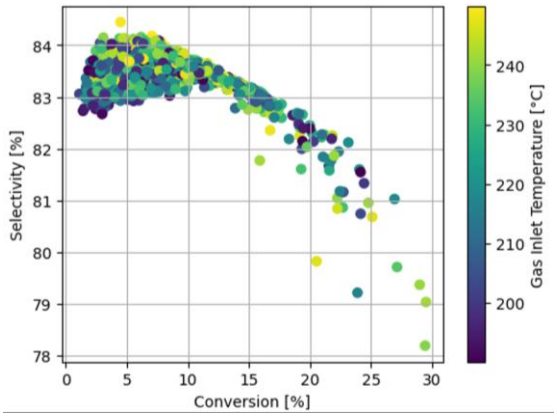

Figure 4.5 – Effect of gas inlet temperature on conversion and selectivity

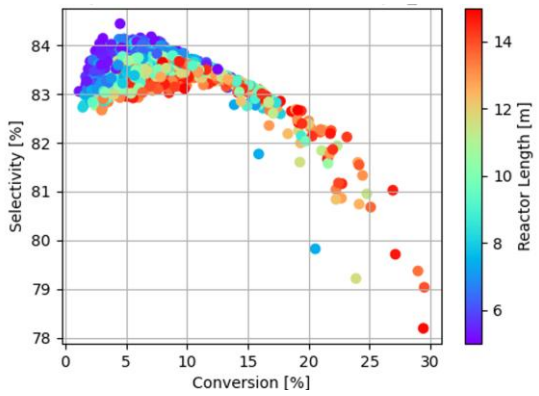

Figure 4.6 – Effect of reactor length on conversion and selectivity

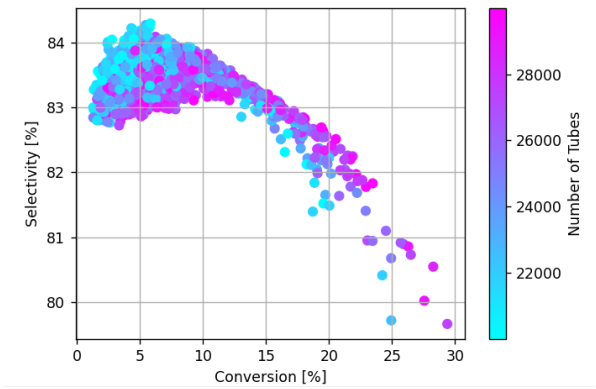

Figure 4.7 – Effect of number of tubes on conversion and selectivity

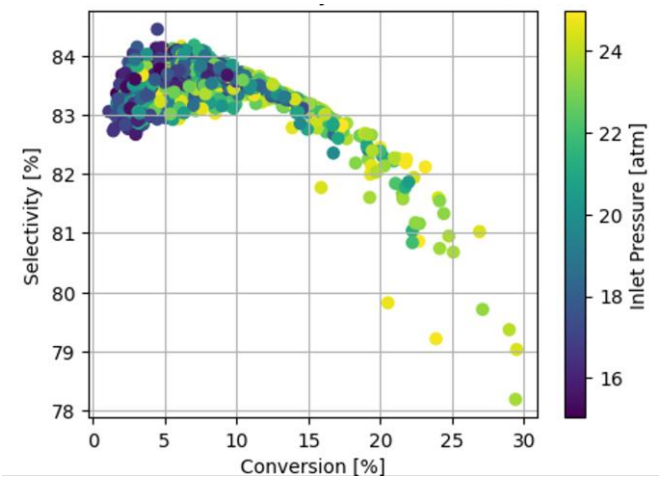

Figure 4.8 – Effect of inlet pressure on conversion and selectivity

Table 4.4 – Summary table of parametric study analysis

Parameter	**Parameter increase effect on selectivity**	**Parameter increase effect on conversion**	**Analysis and key takeaway**
Coolant inlet temperature	Decrease	Increase	Increasing the coolant temperature causes the conversion to increase because a higher temperature leads to faster rate of reaction. However, a decrease in selectivity can also be seen. Therefore, it is crucial to balance the trade of between conversion and selectivity when deciding on the temperature. From the graph it can be seen that temperatures at approximately ~230 °C offer the best trade off (assuming a desired conversion of 10%).

Gas inlet temperature	Insignificant	Insignificant	From the Monte Carlo simulation, it seems as though the gas inlet temperature has no effect. However, this can be explained by the fact that the coolant temperature has much greater effect on the temperature within the reactor than the inlet gas temperature. This result also shows some variation in inlet temperature is acceptable as long as the coolant temperature is set correctly. Further study with a fixed coolant temperature may reveal an optimal temperature range.
Reactor length	Decrease	Increase	A longer reactor has a higher conversion as the residence time increases. However, the selectivity decreases as the reactor length is increased. This can be explained by the fact the undesired EO oxidation reaction is a series reaction, so longer residence time leads to more time for the undesired reaction to occur. From the graph an optimal reactor length can be seen to be around 8 m long (assuming a desired conversion of 10%)
Number of tubes	Decrease	Increase	The trend for this case is the same as the varying reactor length case. This can also be explained the same way as the reactor length case as increasing the number of tubes also increases the residence time. There doesn't seem to be a clear optimal value as it is possible for designs with low or high number of tubes to reach a good selectivity and selection. This shows that the optimal number of tubes depends heavily on the other variable varied in the study.
Inlet pressure	Decrease	Increase	Increasing the pressure in the reactor leads to greater conversion. This is well known in literature and is also the reason why EO reactor are operated at high pressures. The limit of increasing the pressure even higher is determined by the selectivity which can decrease at higher pressures. There are also safety and capital cost concerns that arise from operating at too high of a pressure. Pressures of about 21 atm seem to be optimal

In conclusion, the coolant inlet temperature and inlet pressure should be considered in a further optimisation study due to their heavy impact on selectivity and conversion. In addition, constraints related to the safety should be included as well as an objective function that considers the capital cost of the reactor to find the balance between conversion and capital cost.

The number of tubes and reactor length should also be included in the optimisation study however it is known that the selectivity will be higher with a shorter residence time, therefore the objective function should also consider the recycle flowrate to account for the higher operating cost that comes with a reduced residence time. Other important factors that determine the optimal reactor length include the pressure drop along the reactor and the material cost per reactor length.

For now, the coolant temperature will be kept a 220 °C and the inlet pressure will be kept at 21 atm for the later parts of this report. The number of tubes and reactor length will also be kept the same as the true optimal value will require the aforementioned optimisation study and the current value already provide a good selectivity and conversion.

5 Ancillary Equipment Design

5.1 Piping

Towler and Sinnott (2012) recommend a gas velocity of 15 – 30 m s^{-1} in piping for gas phase fluid. Based on a feed volumetric flowrate of 16.6 m^3 s^{-1} (using ideal gas law), this would require a pipe cross sectional area between approximately 0.5 – 1 m^2. Assuming a value of 0.75 m^2, a pipe diameter of ~1 m will be required. The ASME B31.3 formula (American Society Of Mechanical Engineers, 2005) in Equation 5.1 was then used to calculate the thickness of the pipe of 9.6 mm. Including mill tolerance (commonly 12.5% for seamless pipe) and practical considerations, one might specify a nominal thickness of 12 mm or a corresponding pipe schedule.

$$t = \frac{P \cdot D}{2(S \cdot E + P \cdot Y)} + A \qquad \text{Equation 5.1}$$

Where t is the required pipe wall thickness (9.6 mm), P = internal design pressure (2.1×10^6 Pa), D = outside diameter of the pipe (1 m), S = allowable stress of the pipe material at the design temperature (1.37×10^8 Pa for stainless steel 316L) , E = weld joint efficiency (assumed 1), Y = coefficient (commonly 0.4 for many steels in typical thickness ranges), A = corrosion allowance (2 mm).

It should be noted that this pipe design is for the reactor effluent therefore 316L Stainless Steel was selected as the appropriate material for construction due to the reactivity of the EO in the stream. The streams upstream of the reactor have negligible EO within them. Therefore, a cheaper material maybe more suitable for the design of the upstream piping, such carbon steel.

5.2 Compressor

In the preliminary design most streams were set to 21 atm. In reality, real process conditions involve pressure drops in upstream equipment. In a full plant flowsheet, the pressure leaving the absorption column or other separation units might be lower than 21 atm, requiring recompression back to the reactor feed pressure.

In this design, for demonstration, the reactor effluent pressure a ~18.4 atm is used as the recycle and upstream compressor pressure. The aim of the compressor is to compress it back to 21 atm (or slightly above to account for additional equipment pressure drops).

The first step of the design is to assume an isentropic compression and use Equation 5.2 to calculate the ideal work per unit mass.

$$w_s = \frac{k}{k-1} R T_1 \left[\left(\frac{P_2}{P_1} \right)^{\frac{k-1}{k}} - 1 \right] \qquad \text{Equation 5.2}$$

The specific heat ratio, k, was calculated as the average weighted value of the mixture at a value of 1.29. Using this value in Equation 5.2 with a temperature of 323 K gives a molar work rate of 343 J mol^{-1}. The total isentropic work requirement for the compressor is therefore 3.02 MW. Assuming an isentropic efficiency of 80%, the actual work requirement for the compressor is calculated to be 3.78 MW.

Using Equation 5.3 the outlet temperature from the compression can be calculated as 332 K or 59 °C.

$$T_2 = T_1 \left(\frac{P_2}{P_1}\right)^{\frac{k-1}{k}} \quad \text{Equation 5.3}$$

Given the relatively low pressure ratio (~1.14) but high flow, a single-stage centrifugal compressor will suffice. Detailed vendor data would confirm the exact design (number of impellers, blade angles, etc.).

5.3 Preheating heat exchanger

Before entering the reactor, the gas feed must be preheated to ~210°C. A heat exchanger, often a shell-and-tube or finned-tube design, can be used, potentially recovering heat from hot reactor effluent or other waste-heat streams in the plant. Given the sizeable gas flowrate (8800 mol s^{-1}, or roughly 16.6 m^3 s^{-1} under certain conditions), a shell-and-tube heat exchanger is typically chosen. The relevant advantages of using a shell-and-tube heat exchanger include:

- Shell-and-tube units can handle high pressures (e.g., 18–21 atm) and large volumetric flows.
- Internal baffles can be used on the shell side to enhance turbulence and heat transfer.
- Tubes can be cleaned or replaced without discarding the entire unit.
- Tube-side or shell-side passes can be adjusted to optimise log-mean temperature difference (LMTD) and approach minimal temperature differences for energy efficiency.

To determine the sizing of the heat exchanger first the duty must be calculated. This is shown in Equation 5.4

$$Q = \dot{m_{\text{gas}}} C_{p,\text{mix}} (T_{\text{out}} - T_{\text{in}}) \quad \text{Equation 5.4}$$

Where $\dot{m_{\text{gas}}}$ = molar flow rate of the gas (mol/s), $C_{p,\text{mix}}$= average heat capacity of the gas mixture (J/(mol·K)), $T_{\text{in}}$and T_{out} are the inlet and outlet temperatures of the gas.

The heat exchanger was then sized using the Log Mean Temperature Difference (LMTD) method given in Equation 5.5.

$$Q = UA\,\Delta T_{LM}\,F \quad \text{Equation 5.5}$$

where U = overall heat-transfer coefficient (W/(m²·K)), A = required heat-transfer area (m²), ΔT_{LM}= log-mean temperature difference (K), F = correction factor (dimensionless).

The log-mean temperature difference is given in Equation 5.6.

$$\Delta T_{\mathrm{lm}} = \frac{\left(T_{\mathrm{hot,in}} - T_{\mathrm{cold,out}}\right) - \left(T_{\mathrm{hot,out}} - T_{\mathrm{cold,in}}\right)}{\ln\left[\frac{T_{\mathrm{hot,in}} - T_{\mathrm{cold,out}}}{T_{\mathrm{hot,out}} - T_{\mathrm{cold,in}}}\right]}$$ Equation 5.6

To calculate the value of U the diameter of the tube and number of tubes is required shown in Equations 3.9 – 3.14, however that is also what we are trying to calculate (A) using equation 5.5. Therefore, an initial estimate of the number of pipes and diameter of pipes is required to calculate the value of U. The area of heat transfer is then calculated using this value. Usually there will be a discrepancy between the two area values. In this case the area needs to be adjusted, and the calculation needs to be iterated until a unifying value is found.

5.4 Boiler

As described earlier, the reactor coolant (e.g., Therminol 55) enters the reactor shell side at ~220 °C and may exit at ~227 °C, depending on the heat load from the exothermic reaction. This exit stream, carrying significant thermal energy, must be cooled back to ~220 °C before recirculating to the reactor. To capitalise on this high-temperature heat, an on-site boiler (often referred to as a waste-heat boiler) can be used to generate steam at moderate-to-high pressure.

Using Equation 5.4, the heat removal duty can be calculated as $Q_{\text{boiler}} \approx 2000 \times 2600 \times 7 = 36.4\ \text{MW}$. assuming a constant coolant heat capacity and flowrate of 2000 kg s^{-1}

A minimum approach temperature of ~10 K between the coolant and steam must be maintained to ensure feasible heat transfer. If the coolant leaves the boiler at ~220 °C, the maximum steam saturation temperature is roughly (220 °C – 10 K) = 210 °C. In steam tables, that corresponds to a steam pressure of about ~19 bara.

To estimate how much steam can be generated, consider the enthalpy of vaporization $(\Delta H_{\mathrm{vap}})$ at 19 bara, plus the sensible heat needed to bring boiler feedwater from its inlet temperature to saturation. For a rough calculation, the boiler feed water was assumed to be 130 °C and the steam generated was not superheated, so kept at 210 °C. The enthalpy of vaporisation at 19 bara is 1900 kJ kg^{-1}. The sensible heat from 130 to 210 °C is approximately 200 kJ kg^{-1}. Therefore, the mass flowrate of steam generated is calculated as

$$\text{Steam flowrate} \approx \frac{36.4 \times 10^{6}\ \mathrm{J\,s^{-1}}}{2100\ \mathrm{J\,g^{-1}}} \approx 17.3\ \mathrm{kg\,s^{-1}} \approx 62{,}280\ \mathrm{kg\,h^{-1}}.$$

The sizing of the boiler will require a similar approach to the one followed in Section 5.3.

6 Mass and Energy Balance

The stream table from Section 1 was updated is presented in Table 6.1. The main changes in the stream table include the inlet temperature to the reactor (stream 13), the reactor effluent conditions and composition (stream 14) and the pressure of the streams upstream the compressor C-101.

Table 6.1 – updated mass and energy balance

Stream	8	9	10	11	12	13 (Feed)	14	32
Vapour Mole Fraction	1	1	1	1	1	1	1	1
Temperature (^{O}C)	50	50	50	59	59	210	229	64
Pressure (atm)	18.4	18.4	18.4	18.4	21	21	18.4	18.4
Molar Flowrate (mol s^{-1})	142	167	56	8800	8800	8800	8743	8444
Molar Enthalpy (kJ/kmol)	730	1300	900	1280	1280	7000	7700	1470
Molar Fraction								
C2H4	0	1	0	0.173	0.173	0.173	0.156	0.161
EO	0	0	0	0.00001	0.00001	0.00001	0.015	0.00001
CH4	0	0	1	0.675	0.675	0.675	0.679	0.697
CO2	0	0	0	0.029	0.029	0.029	0.035	0.03
H2O	0	0	0	0.005	0.005	0.005	0.011	0.006
Ar	0.02	0	0	0.035	0.035	0.035	0.035	0.036
O2	0.98	0	0	0.084	0.084	0.084	0.069	0.071

7 Material Selection and Mechanical Design

This section focuses on the materials selection, internal design features, key mechanical sizing, and specification sheets for the principal equipment in the ethylene oxide (EO) production plant. Emphasis is placed on the reactor, piping, and critical ancillary equipment (e.g., boiler, heat exchangers) that must withstand the specified operating conditions while ensuring safety, reliability, and economic feasibility.

7.1 Materials Selection

A key objective in selecting materials for an ethylene oxide (EO) production plant is ensuring that all construction components can withstand the combination of temperature, pressure, and chemical reactivity inherent to EO synthesis. The primary considerations include corrosion resistance, mechanical strength under pressurized and high-temperature conditions, and compatibility with ethylene oxide and other process fluids. Industry standards (ASME) guide these decisions, as safety and reliability are paramount in managing an exothermic partial-oxidation reaction.

7.1.1 Criteria for Material Choice

Corrosion resistance stands at the forefront of material requirements because ethylene oxide

can readily react with certain metals or form unwanted byproducts. In the presence of oxygen and temperatures up to about 230 °C, lesser alloys may corrode, suffer pitting, or catalyse side reactions leading to polymerization. Mechanical properties must also be sufficient to handle operating pressures near 18–22 atm, necessitating adequate tensile and yield strength to ensure integrity over time. Equally important, the material must not introduce contaminants that could prompt explosive reactions; for instance, metals such as copper or zinc can form acetylides in contact with acetylenic impurities, posing an ignition risk.

These constraints point to stainless steels—especially grades 304L and 316L—as the dominant choice for surfaces exposed directly to ethylene oxide or its intermediates. Their oxide-rich surface layers and alloying elements (notably chromium, nickel, and molybdenum) enhance corrosion resistance and reduce the likelihood of catalytic polymerisation or decomposition. Even so, different areas of the plant may demand varying levels of corrosion and thermal protection; hence, the material selection for each component should align with its anticipated service conditions.

7.1.2 Selected Materials

For the high-pressure, high-temperature environment inside the reactor tubes, 316L stainless steel is typically chosen. Its molybdenum content offers improved resistance to pitting and crevice corrosion, which is critical in preventing localised degradation under EO service. The reactor shell can be constructed of carbon steel if the coolant is benign (e.g., a heat-transfer fluid such as Therminol).

Streams containing ethylene oxide generally require 316L stainless steel piping due to EO’s reactive nature. In contrast, carbon steel is sufficient for lines carrying minimal or no EO, such as many feed and utility lines. The final thickness and schedule for each line follow ASME B31.3 guidelines, factoring in design temperature, pressure, and a suitable corrosion allowance.

Because the steam-generation section typically encounters only heat-transfer fluid and water/steam, carbon steel or low-alloy steel is a cost-effective choice that can handle moderate temperatures and pressures.

Streams upstream of the reactor contain negligible EO, so carbon steel tubes generally suffice, with corrosion allowances considered for any contaminants. If future operational changes introduce more aggressive conditions, higher-alloy steels could be specified.

7.2 Design of Internals

7.2.1 Design Basis and Assumptions

The tube side of the reactor is where the high pressure mixture will be flowing. The operating pressure is approximately 21 atm. Therefore, a reasonable design pressure of 25 bar will be used for calculating the required thickness of the tubes. Although the process operates at about 230 °C within the reactor, during actual operation the temperature of the gas needs to be increased to account for the catalyst deactivation that occurs. As a result, the design temperature will be assumed to be 300 °C.

7.2.2 Tube thickness and weight

The ASME B31.3 equation (Equation 7.1) for pipes is used for calculating the thickness of tube in this case.

$$t_{\text{tube}} = \frac{P\,D_{\text{in}}}{2\,(S\,E + P\,Y)} + \text{CA} \qquad \text{Equation 7.1}$$

Given that the design pressure is $P = 2.5 \times 10^6\ \text{Pa}$, the required internal diameter $D_{\text{in}} = 0.045\ \text{m}$, the allowable stress of 316L Stainless Steel at 300 °C $S = 7.25 \times 10^7\ \text{Pa}$ and assuming a joint efficiency of $E = 1.0$, a code factor $Y = 0.4$, and a corrosion allowance of 1mm. The tube thickness requirement is approximately 1.4 mm. this can be rounded up to 2 mm to accommodate tolerances.

The weight of the all the tubes is equal to the product of the circumference, tube thickness, tube length, number of tube and density of stainless steel. The total mass of the tubes was 895 tonnes.

7.2.3 Stress

The hoop stress can be calculated using Equation 7.2

$$\sigma_{\text{hoop}} = \frac{P\,r}{t} \qquad \text{Equation 7.2}$$

Using this equation, a hoop stress of 28.125 MPa was calculated for a tube. The longitudinal stress does need to be calculated as there is no force being applied in that direction.

7.2.4 Catalyst and inert packing weight

The mass of catalyst and inert required is calculated in this section. First the volume of catalyst was determined by multiplying the cross sectional area of the tube ($1.59 \times 10^{-3}\ m^2$), the solid fraction (0.55) and the length of the catalyst section (12 m) in the reactor. The calculated volume per tube was then multiplied by the number of tubes (25000) to give a final volume requirement of catalysts of 262.3 m^3. This value was then multiplied by the density of the catalyst 1260 kg m^3 to give a mass of 331 tonnes

The calculation of the weight of inert used the same process except a length of 2 m was used and the density of the inert was assumed to be 1200 kg m^3, the typical value for ceramic. This gave a total mass of inert packing of 25.9 tonnes.

7.3 Key Mechanical Design

7.3.1 Design Basis and assumptions

The shell side of the reactor operates at a lower pressure than the tube side due to the lower pressure requirement for the coolant. A design pressure of 5 bar was assumed for the shell side. Given that the temperature of the coolant is gradually increased over the operation of the reactor to counteract the effect of catalyst deactivation, the highest temperature should be used for the design temperature. For this case a design temperature of 300 °C was assumed. The vessel is designed as horizontal cylinder with semi ellipsoidal heads, supported by saddles.

7.3.2 Shell side wall thickness

For a cylindrical shell under internal pressure, a widely used ASME Section VIII Div. 1 formula is given in Equation 7.3

$$t = \frac{P\,R}{S\,E - 0.6\,P} + \mathrm{CA}, \qquad \text{Equation 7.3}$$

Where t = required shell thickness (m), P= internal design pressure (5x10^5 Pa), R = inside radius of the cylinder (8 m), S= allowable stress at design temperature for carbon steel SA 516-60 at 300 °C (115 x10^6 Pa), E= weld joint efficiency (dimensionless), CA = corrosion allowance (m)

For the packed bed reactor, the shell thickness will be calculated as:

$$t = \frac{5 \times 10^5 \times 4.0}{5 \times 10^8} = 0.00738\ \mathrm{m}.$$

Rounding up to include corrosion allowance and other tolerance the thickness of the wall should at minimum be 10 mm.

The thickness of the semi-ellipsoidal heads can be calculated from Equation 7.4

$$t = \frac{P\,D_I}{2\,\mathrm{S}\,\mathrm{E} - 0.2\,P} + CA \qquad \text{Equation 7.4}$$

Using this equation a value of 11 mm was calculated given that carbon steel has a maximum allowable stress of 115 MPa at 300 °C and a corrosion allowance of 2 mm was used.

7.3.3 Stress

The longitudinal stress and hoop stress can be calculated as

$$\sigma_l = \frac{P\,D}{4t} = 90.9\ \mathrm{MPa} \qquad \text{Equation 7.5}$$

$$\sigma_h = \frac{P\,D}{2t} = 181.8\ \mathrm{MPa} \qquad \text{Equation 7.6}$$

7.3.4 Insulation

Insulation isn't required for the vessel as cooling is desired due to the exothermic nature of the reactor.

7.3.5 Dead weight load of entire vessel

The mass of the vessel can be estimated by summing the contributions of the shell, the heads, and any additional internals. For the shell and head components, the basic approach is to calculate the surface area, multiply by the respective wall thickness, and then multiply by the material density. For carbon steel (density ≈ 7850 kg/m³), the calculations are as follows:

Shell Mass

The lateral surface area is given by

$$A_{cyl} = 2\pi RL = 2\pi(4.0\ \mathrm{m})(14\ \mathrm{m}) \approx 351.9\ \mathrm{m}^2$$

where R is the inside radius (4 m) and L is the length of the cylindrical section (14 m). The mass is then

$$M_{shell} = A_{cyl}\, t\, \rho \; = 351.9\,\text{m}^2 \times 0.01\,\text{m} \times 7850\,\text{kg/m}^3 \approx 30,386\,\text{kg}$$

where t is the wall thickness (10 mm = 0.01 m) and ρ is the density.

Head Mass

The effective area of each head can be estimated using geometrical relations for ellipsoids. For simplicity, one may approximate each head's area as similar to a hemispherical shape Using the calculated thickness (11 mm) and the same material density, the mass of both heads is computed similarly by

$$A_{\text{hemi}} = 2\pi(4.0\,\text{m})^2 = 2\pi \times 16 = 32\pi \approx 100.53\,\text{m}^2$$

$$A_{\text{heads}} = 2 \times 100.53\,\text{m}^2 \approx 201.06\,\text{m}^2$$

$$M_{\text{heads}} = A_{heads}\, t_{head}\, \rho = 201.06\,\text{m}^2 \times 0.011\,\text{m} \times 7850\,\text{kg/m}^3 \approx 17{,}341\,\text{kg}$$

where A_{heads} is the combined surface area of the two heads and t_{head} is the chosen head wall thickness.

7.3.6 Total Vessel Mass

Adding these components gives

$$M_{\text{total}} = 331{,}000\,\text{kg} \; + \; 26{,}000\,\text{kg} \; + \; 64{,}000\,\text{kg} + 17{,}500\,\text{kg} + 8{,}100\,\text{kg} \approx 446{,}600\,\text{kg}$$

7.3.7 Standard Specification Sheet

Group MA
Freeport industrial park lot 3

FIXED BED REACTOR

Form XXXXX-YY-ZZ

Project Name
Project Number Sheet 1 of 1

REV	DATE	BY	APVD	REV	DATE	BY	APVD

Owner's Name	Ammar Ali						
Plant Location	Texas USA					Units	○ English ◉ Metric
Case Description							
Equipment label	R-101	Equipment name	Multi tubular packed bed reactor				
Plant section	Section 1						
Process service							
Design code	ASME	Maximum diameter	10 m	Total height	15	m	

PROCESS DATA

Bed Number		1
Gas flow direction		Up
Coolant flow direction		Up
Operating temperature	°C	230
Pressure	bara	21
Gas flow	kg/h	27
Gas density	kg/m3	11
Gas dynamic viscosity	N.s/m2	1.62E-05
Cool flow	kg/h	7.20E+06
Cool density	kg/m3	734
Cool dynamic viscosity	N.s/m2	6.30E-04
Catalyst type		Silver
Catalyst shape		sphere
Catalyst nominal diameter	mm	6
Catalyst bed depth	m	12
Catalyst volume	m3	8.58E-03
Catalyst bed bulk density	kg/m3	1260
Catalyst bed void fraction		0.45
Catalyst support		Alumnia oxide
GHSV	/h	2034
Notes		

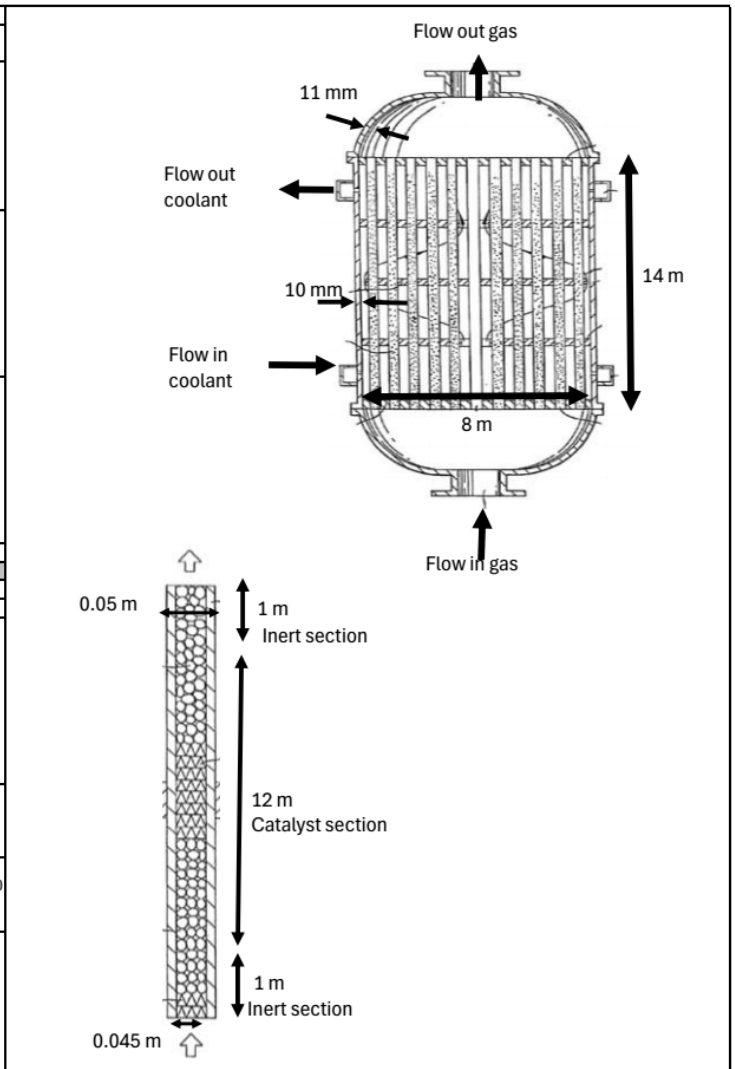

CONSTRUCTION & MATERIALS

Bed Number		
Shell material		Stainless Steel
Shell diameter	m	8
Shell tangent length	m	14
Shell thickness	mm	7.5
Design temperature	°C	300
Design pressure	bara	5
Test pressure	bara	4
Head shape		Hemi spherical
Head thickness	mm	11
Tube internal diameter	mm	0.045
Tube outer diameter	mm	0.05
Catalyst length of tube	m	12
inert length of tube	m	1
Inert material		Ceramic
Shell material		Carbon S SA 516-60
Tube material		Stainless steel 316L
Shell thickness	mm	10
Notes		

8 Process Control and Safety Considerations

Reliable control of the ethylene oxide reactor relies on maintaining several key process variables in the correct ranges. In particular, careful management of inlet pressure, oxygen concentration, coolant temperature, and overall reactor temperature is critical to ensure high selectivity, stable operation, and prevention of hazardous conditions. This section outlines the primary control loops and describes the central safety systems and interlocks that protect against thermal runaway and flammable mixtures.

8.1 Key Variables for Control

The first variable requiring close regulation is the oxygen concentration entering the reactor. Ullmann and Gerhartz (1995) the importance of holding O_2 levels below about 9 mol % to avoid flammability risks and excessive oxidation side reactions. The second variable is the coolant temperature based on the parametric study results, which showed how it strongly influences the reactor's selectivity to ethylene oxide because higher temperature differentials can either remove heat too aggressively or insufficiently, affecting the catalyst performance. Another key parameter is the inlet pressure on the tube side, typically around 21 atm, which drives the reaction rate and overall selectivity. Controlling it near the desired setpoint prevents undesirable drops or surges in conversion. The reactor bed temperature itself is also critical, both as an indicator of hot spots and a determinant of reaction kinetics. This temperature must be tracked along the length of the catalyst bed or, in larger reactors, at multiple points to identify local deviations that might indicate the onset of runaway.

8.2 Control Strategy and P&ID References

Each of these variables is managed by a corresponding control loop. An illustrative P&ID, shown Section 8.5, depicts the principal instruments and controllers:

1. O_2 Flow Control uses an oxygen analyser on the feed line to ensure that the partial pressure of oxygen remains within the safe range for partial oxidation. A flow transmitter (FT-102) and flow controller (FIC-102) modulate the control valve (FCV-102) on the oxygen feed. If the analyser AT-101 reads an oxygen fraction above the target, the controller reduces the valve opening to bring the composition back into line.

2. Coolant temperature control relies on a temperature transmitter (TT-105) placed in or near the reactor tubes, feeding a temperature controller (TIC-103) that manipulates the set point of TIC-102 which controls the control valve (TCV) on the coolant circuit. This controller can adjust the flow or temperature of the incoming coolant, thereby removing or supplying heat to match the reactor's exothermic load. It is desirable to have tight control of the reactor temperature, therefore it was deemed necessary to implement a cascade control system which uses the temperature of the coolant.

3. Inlet pressure control centres on a pressure transmitter (PT-104) installed upstream of the reactor tubes. The pressure controller (PIC-101) manages the recycle valve to ensure the reactor feed remains at approximately 21 atm. If the reactor pressure drops, the controller signals close the reactor effluent valve to boost the inlet pressure, while high-pressure readings prompt the effluent control valve to open, reducing pressure.

This integrated scheme ensures that each major parameter identified by the parametric study and oxygen concentration remains stable. By referencing the P&ID, operators can quickly verify each control loop's function, including the relevant setpoints, alarm thresholds, and final control elements.

8.3 Safety Systems and Interlocks

Safety considerations revolve around preventing runaway reactions and avoiding explosive mixtures of ethylene and oxygen. One of the most important protective measures is a high-temperature trip that automatically closes feed valves if the bed temperature exceeds a maximum allowable limit. This interlock defends against localised overheating that can drastically reduce catalyst selectivity and endanger mechanical integrity.

In addition, an oxygen analyzer interlock halts or diverts oxygen flow if the measured concentration in the feed rises above the safe threshold. This is typically implemented as a “hardwired” emergency shutdown (ESD) function so that no software or network delays can compromise its activation. An emergency depressurization system, often a spring-loaded or pilot-operated relief valve network, helps release reactor pressure safely to a flare or vent system if abnormal conditions persist or if the main feed valves fail to close.

Instrumentation for detecting combustible gases or oxygen leaks should also deployed around the reactor and associated piping. If a flammable mixture is detected in the plant environment, a plant-wide alarm and general evacuation procedure can be initiated. These detectors are usually placed near potential leak points, such as compressor seals, major flanges, and valves.

8.4 Summary of Controllers and Valves

The main items of instrumentation and control that appear on the P&ID include the following:

- Flow Controllers (FIC) for ethylene, oxygen, and recycle lines to ensure stable feed ratios. Each flow controller has a corresponding flow transmitter (FT) and a pneumatically or electrically actuated control valve (FV).
- Temperature Controller (TIC) connected to bed temperature sensors (TT) and the coolant flow valve (CV). By continuously adjusting coolant flow or temperature, this loop limits reactor temperature fluctuations.
- Pressure Controller (PIC) referencing a pressure transmitter (PT) at the reactor inlet and manipulating either a recycle valve or compressor speed. This keeps the feed pressure near the desired setpoint.

These controllers, valves, and safety systems form a multi-layer protective framework. The coordinated interplay of basic regulatory loops and emergency interlocks upholds both the production targets, as indicated by the parametric study, and the stringent safety standards demanded in EO service. By ensuring accurate measurement, swift response, and robust fail-safe mechanisms, the ethylene oxide reactor can operate efficiently, maintaining conversion and selectivity without compromising on plant safety.

8.5 P&ID

Notes:

1. Symbol are standard P&ID symbols
2. TSL – to a safe location
3. FT, FIC,FY, FCV – Flow transmitter, Flow Indicator Controller, Flow ratio, Flow Control Valve
4. PT, PIC, PCV, PC – Pressure Transmitter, Pressure Indicator Controller, Pressure Control Valve, Pressure Controller
5. TT, TIC, TCV, - Temperature Transmitter, Temperature Indicator Controller, Temperature Control Valve.
6. ST, SIC, SCV – Speed Transmitter, Speed Indicator Controller, Speed Control Valve.
7. ASC – Anti Surge Controller
8. SP – Set point

Revision No	Revision notes	Date	Drawing by	Check by
1		1/2/33	A Ali	B Ali
Group MA : Section 1 Ethylene Oxide Plant				

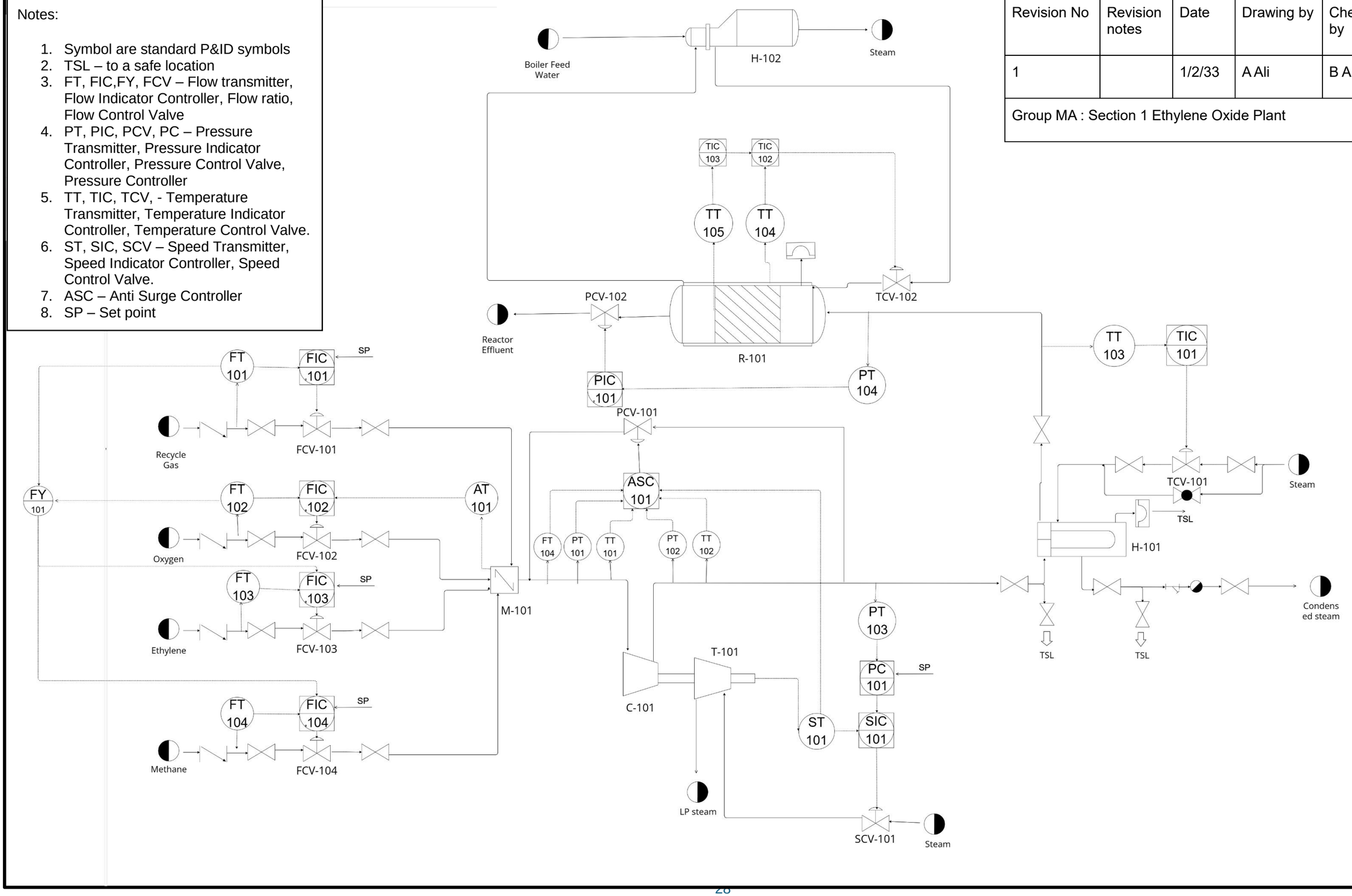

9 Conclusion

The ethylene oxide reactor system presented in this report reflects a balance among critical design drivers: safe, efficient heat removal for an exothermic and potentially hazardous reaction; robust handling of oxygen-rich feeds at elevated pressures; and maintenance of high selectivity to ethylene oxide through prudent operating conditions and the controlled use of an inhibitor. The multi-tubular packed-bed arrangement, with numerous tubes packed with a silver-based catalyst, meets industrial requirements for managing heat release while achieving moderate single-pass conversions of 10% at selectivities of about 84%. This approach enables a reliable and comparatively simpler design, in which excess ethylene is recycled to sustain high overall yields.

The kinetic model and parametric studies highlight the interdependence of oxygen partial pressure, coolant temperature, and inhibitor concentration in optimising ethylene oxide selectivity. Maintaining a careful compromise in these variables allows the reactor to avoid runaway regimes and to minimise the secondary oxidation of ethylene oxide to carbon dioxide. Mechanical design calculations confirm that the chosen tube and shell dimensions, alloy specifications, and thicknesses are consistent with ASME standards, offering adequate strength to handle pressures around twenty bar and design temperatures up to three hundred degrees Celsius.

Downstream ancillary equipment, including the required piping, compressor, preheater, and waste-heat boiler, is suitably sized to manage large volumetric flow rates, recycle streams, and effective heat recovery. The mass and energy balances, along with the mechanical design calculations, remain aligned with typical industrial practice, with design pressures and temperatures comfortably within safe operating margins.

Process control considerations emphasise the tight regulation of coolant temperature, reactor bed temperature, and oxygen feed to avoid flammable or runaway conditions. A robust system of emergency shutdowns, interlocks, and continuous inhibitor dosing further ensures stable operations and preserves catalyst life.

Overall, the final design stands on established industry practice for EO production, coupling moderate per-pass conversions with high recycle to enhance selectivity and yield. The multi-tubular reactor configuration with a carefully tailored catalyst, effective inhibitor usage, and reliable cooling strategy demonstrates a proven and economical path to ethylene oxide production at the anticipated scale.

Despite its strengths, several improvements could increase both the reactor’s performance and the accuracy of the design. For example, while the current model approximates each tube as a one-dimensional plug flow, future work may investigate radial temperature or concentration gradients, especially near the hotspot region. Including detailed catalyst-pore diffusion effects or advanced geometry (e.g. ring- or multi-hole pellets) could yield more accurate reaction rate profiles.

In addition, the present design only focuses on start-of-run activity. An explicit model of catalyst aging, perhaps incorporating empirical deactivation kinetics or chlorine balance, would help plan for temperature ramp and end-of-run operation. This foresight could also show how best to adjust inhibitor feed over the catalyst’s lifespan.

The creation of a dynamic model would allow an analysis of the reactor operation with real-time feedback on bed temperatures, EO concentration, and oxygen partial pressure. This

could enable advanced feed-forward or model-predictive control strategies that seamlessly adjust inhibitor injection and coolant flowrate. Such strategies would continually adapt to day-to-day catalyst variations and shifting production targets, maintaining near-optimal conversion and selectivity.

By incorporating these potential upgrades, the overall accuracy, safety, and efficiency of the ethylene oxide reactor design could be further improved. Nonetheless, the present solution stands on established industrial practice and delivers a comprehensive, economically viable approach to EO production with high selectivity and robust safety safeguards.

References

American Society Of Mechanical Engineers (2005). *Process piping : ASME code for pressure piping, B31.* New York: American Society Of Mechanical Engineers.

Aryana, S., Ahmadi, M., Gomes, V.G., Romagnoli, J.A. and Ngian, K. (2009). Modelling and Optimisation of an Industrial Ethylene Oxide Reactor. *Chemical Product and Process Modeling*, 4(1). doi:https://doi.org/10.2202/1934-2659.1231.

Barecka, M.H., Skiborowski, M. and Górak, A. (2017). A novel approach for process retrofitting through process intensification: Ethylene oxide case study. *Chemical Engineering Research and Design*, 123, pp.295–316. doi:https://doi.org/10.1016/j.cherd.2017.05.014.

Berg, V. (2025). Selective Oxidation of Ethylene to Ethylene Oxide on Silver Catalysts at Industrial Conditions: Reactor Profiles, Kinetics and Chlorine Inhibition. doi:https://doi.org/10.15480/882.14136.

Eastman Chemical Company (2015). Therminol 55 Heat Transfer Fluid Physical and Chemical Characteristics.

Fazeli, A., Naseri, A. and Eslamjamal, F. (2020). Kinetic Models of Ethylene Oxide Production on Ag Catalysts: A Review. *Kinetics and Catalysis*, 61(4), pp.603–612. doi:https://doi.org/10.1134/s0023158420040059.

Galan, O., Gomes, V.G., Romagnoli, J. and Ngian, K.F. (2009). Selective Oxidation of Ethylene in an Industrial Packed-Bed Reactor: Modelling, Analysis and Optimization. *International Journal of Chemical Reactor Engineering*, 7(1). doi:https://doi.org/10.2202/1542-6580.2058.

H Scott Fogler (2018). *Essentials of chemical reaction engineering*. 2nd ed. Harlow Prentice Hall.

Kirk, R.E. and Othmer, D.F. (2005). *Encyclopedia of chemical technology*. New York ; Chichester: Wiley.

National Institute of Standards and Technology (1997). *NIST Chemistry WebBook - SRD 69*. [online] NIST. Available at: https://webbook.nist.gov/chemistry/.

National Institute Of Standards And Technology (U.S (1990). *Nist.* Gaithersburg, Md.: U.S. Dept. Of Commerce, National Institute Of Standards And Technology.

Nawaz, Z. (2016). Heterogeneous Reactor Modeling of an Industrial Multitubular Packed-Bed Ethylene Oxide Reactor. *Chemical Engineering & Technology*, 39(10), pp.1845–1857. doi:https://doi.org/10.1002/ceat.201500603.

Perzon, H. (2015). *A Simulation Model of a reactor for Ethylene Oxide production*.

Peschel, A., Karst, F., Freund, H. and Sundmacher, K. (2011). Analysis and optimal design of an ethylene oxide reactor. *Chemical Engineering Science*, 66(24), pp.6453–6469. doi:https://doi.org/10.1016/j.ces.2011.08.054.

Petrov, L., Eliyas, A., Maximov, C. and Shopov, D. (1988). Ethylene oxide oxidation over a supported silver catalyst: I. Kinetics of uninhibited oxidation. *Applied Catalysis*, [online] 41, pp.23–38. doi:https://doi.org/10.1016/S0166-9834(00)80379-6.

Petrov, L., Eliyas, A. and Shopov, D. (1985). A kinetic model of steady state ethylene epoxidation over a supported silver catalyst. *Applied Catalysis*, 18(1), pp.87–103. doi:https://doi.org/10.1016/s0166-9834(00)80301-2.

Petrov, L., Eliyas, A. and Shopov, D. (1986). Kinetics of ethylene oxidation over a silver catalyst in the presence of dichloroethane. *Applied Catalysis*, 24(1-2), pp.145–161. doi:https://doi.org/10.1016/s0166-9834(00)81264-6.

Piccinini, N. and Levy, G. (1984). Ethylene oxide reactor: Safety according to operability analysis. *The Canadian Journal of Chemical Engineering*, 62(4), pp.547–558. doi:https://doi.org/10.1002/cjce.5450620415.

Poling, B.E., Prausnitz, J.M. and John Paul O'connell (2007). *The properties of gases and liquids*. Boston: Mcgraw-Hill, Cop.

S. Kim, C. (1975). *Thermophysical Properties of Stainless Steels*. Argonne National Laboratory.

Salmi, T., Roche, M., Hernández Carucci, J., Eränen, K. and Murzin, D. (2012). Ethylene oxide – kinetics and mechanism. *Current Opinion in Chemical Engineering*, 1(3), pp.321–327. doi:https://doi.org/10.1016/j.coche.2012.06.002.

Shi, Y., Chen, H., Chen, W., Ye, G., Qu, J., Li, J., Zhou, X. and Duan, X. (2023). Effects of particle shape and packing style on ethylene oxidation reaction using particle-resolved CFD simulation. *Particuology*, 82, pp.87–97. doi:https://doi.org/10.1016/j.partic.2023.01.012.

Smith, R. (2016). *Chemical Process Design and Integration, 2nd Edition.* John Wiley & Sons.

Smith, R. (2022). *Process Plant Design*. Wiley-Blackwell.

Towler, G. and Sinnott, R.K. (2012). *Chemical Engineering Design : Principles, Practice and Economics of Plant and Process Design*. 2nd ed. Burlington: Elsevier Science.

Ullmann, F. and Gerhartz, W. (1995). *Ullmann's Encyclopedia of Industrial Chemistry*. Wiley-VCH.

Vandervoort, A., Thibault, J. and Gupta, Y.P. (2011). Multi-Objective Optimization of an Ethylene Oxide Reactor. *International Journal of Chemical Reactor Engineering*, 9(1). doi:https://doi.org/10.1515/1542-6580.2548.

Welty, J.R. and Al, E. (2008). *Fundamentals of momentum, heat, and mass transfer*. Hoboken, N.J.: Wiley ; Chichester.

White, F.M. (2006). *Viscous fluid flow*. Boston ; Montreal: Mcgraw-Hill Higher Education.

Zhou, X.-G. and Yuan, W.-K. (2005). Optimization of the fixed-bed reactor for ethylene epoxidation. *Chemical Engineering and Processing: Process Intensification*, 44(10), pp.1098–1107. doi:https://doi.org/10.1016/j.cep.2005.03.008.